IJL, Issue 2, Vol. 23, 2024
https://doi.org/10.31900/ijl.v23i2.493

Research Article

Simulation design of Photonic Crystal Fiber Temperature sensor based on Surface Plasmon Resonance

Namaa Salem Rahim*, Soudad S. Ahmed

Department of physics, college of science, university of Baghdad, Baghdad, Iraq
** Email address of the Corresponding Author:namaasalem652@gmail.com*

Article history: Received 22 Jul. 2024; Revised 14 Aug. 2024; Accepted 27 Aug. 2024; Published online 15 Dec. 2024

Abstract: Photonic crystal fiber (PCF) sensors based on surface Plasmon resonance with a gold layer coating are prepared and studied in this paper for detecting environmental temperature. A finite element method is utilized to increase the critical geometry parameter. An air hole on the right side of the PCF core is covered utilizing a gold metal that has a thickness of 50nm. PCF cores with circular air holes coated in gold and filled with water samples had considerable confinement losses in the y-polarization direction. When the temperature rises from 48 °C to 75 °C the RI of water will reduce. Numerical analysis of the suggested sensor was conducted utilizing FEM. Simulation using the COMSOL software was used to estimate performance parameters such as amplitude sensitivity, wavelength sensitivity, and resolution. Results indicate that the air hole covered with (Au) acts as a (SPR) sensing feed to sense the RI of water. In the sensing range (1.32-1.3266), amplitude sensitivity S_A was 422.154 RIU^{-1} and maximum resolution was $2.75 * 10^{-5}$ RIU.

Keywords: Optical Fiber Sensor, Surface Plasmon Resonance(SPR), Photonic Crystal Fiber(PCF), Temperature Sensor, Fabry–Perot interferometer.

1. Introduction

As a consequence of their heightened sensitivity in noticing different biological and chemical elements, SPR fiber sensors have evolved into a desirable study subject in modern years. These fiber sensors have tremendous potential in biomedical and life safety applications [1]. Besides being small, it is also electrically passive, stronger, and has a fast optical reaction, which reduces electromagnetic interference. [2]. in the last 20 years, fiber manufacturing technology has improved significantly. The remarkable characteristics of PCFs that cannot be achieved by conventional optical fibers have attracted a lot of attention in recent years. They are small, which decreases electromagnetic interference, and increases sensitiveness, electrical passiveness, and strength [3]. PCFs differ from traditional optical fibers by having low dispersion, and high reflectivity. The PCF's amazing technique substantially enhances single-mode detention by putting considerable air-filled holes along its length [4] Unlike optical fiber, PCF throughout the cladding part a finite number of holes are distributed along the fiber axis [5-7]. The effect of (PCFs)

contain revealed the possible integrity of optical fibers in biological and chemical detection [8, 9]. The optical fiber-based SPR notices multiple topics of good; for instance, enhanced and elastic optical design, promotion of remote sensing, and continued study [10- 12]. SPR can easily be observed in PCFs, and the sensor can be measured by varying the fiber's factors (pitch size, air hole radius, etc.). Whether the metal covering is deposited within the PCF air holes or on the PCF's outer surface, an SPR effect is generated. There have been extensive studies of SPR sensors using numerous plasmonic materials, excluding copper, gold, and silver [13, 14]. The utilization of optical fiber (SPR) was first obtainable in 1993[15]. In SPR, free electrons inside the metallic film interact with light. During resonance, the energy of light reflected off a metal film drops ominously if electron oscillation frequency matches incident light frequency. The metal layer transmits photon energy to form a Plasmon wave on the surface [16,17].to excite the SPR optical instruments like a diffraction grating, optical fiber, and refractive index prism are operated [18]. At the interface, plasma oscillations are localized. A Plasmon is a representation of plasma frequency established on a quasi-particle [19]. Plasma oscillation signifies that free electrons of the metal oscillate from their equilibrium position [20, 21]. The resonance form depends on the dielectric constant of individually the metal and the dielectric [22]. The SPR result is sensitive to differences in the RI on the metal cover [23, 24]. Various investigations have benefited from the PCF-SPR detector [25-27]. (SPR) established temperature sensors are important because of their increased sensitivity, suitable process, and label-free dimension abilities [28]. The main materials utilized in SPR are aluminum, silver, copper, and gold [29]. Silver and gold are widely utilized as a plasmonic material [30]. Numerous of the PCF-established SPR sensors utilize Au as the Plasmonic quantifiable. Gold is chemically fixed [31]. In this investigation, nevertheless, the sensor implementation was greatly enhanced by utilizing an inner sensing technique. Accordingly, performing sufficient pairing between the SPP mode and the core-guiding mode can enhance the sensor's implementation. Numerous registers of this sensor have been mathematically analyzed, and the prevalence of documented PCF is complex to manufacture due to difficult design and small fiber diameter. The FEM was utilized to analyze PCF established on SPR in this investigation. The simulated PCF's cross-section shows a solid core enclosed by six regular arrays of air holes. The right side of the solid core is covered by gold, and occupied by water. The suggested design performs maximum sensitivity, containing sensor resolution and amplitude sensitivity. The configuration that was presented was very sensitive, constructing it an excellent component for measuring and sensing the temperature of the surrounding environment.

2. Theoretical investigation and design of sensors

A. Sellmeier Equation

The silica is used in the building of the proposed sensor. The arrangement's holes are empty, or filled with air. To calculate the RI of silica, the Sellmeier equation is applied [2]:

$$N_{silica} = 1 + \frac{a_1 \lambda^2}{\lambda^2 - b_1} + \frac{a_2 \lambda^2}{\lambda^2 - b_2} + \frac{a_3 \lambda^2}{\lambda^2 - b_3} \quad (1)$$

Where: N is the refractive index of silica, which changes depending on the wavelength, λ is the wavelength, and Sellmeier coefficients are (a_1 , a_2, a_3) and (b_1, b_2, b_3), where a_1 =0.6961663, a_2 =0.4079426, a_3 = 0.8974794, b_1=0.0684043μm^2, b_2= 0.1162414 μm^{2}and b_2=9.896161μm^2.

B. Drude–Lorentz Model

For determining the real and imaginary components of the dielectric constant (ε) at a higher frequency, the Drude model is not appropriate. A totality of Lorentzian functions can nullify the interband effect (IB). Accordingly, a dielectric function can be expressed as $\varepsilon(\omega) = \varepsilon Drude(\omega) + \varepsilon IB(\omega)$ [2]. The Drude-Lorentz model estimates Au's material distribution as

$$\varepsilon_{Au} = \varepsilon_{\alpha} - \frac{\omega_D^2}{\omega(\omega + j\gamma_{D)}} - \frac{\Delta\varepsilon.\Omega_L^2}{(\omega^2 - \Omega_L^2) + j\Gamma_L\omega} \quad (2)$$

Where: $\varepsilon Drude\ (\omega)$ is the relative Permittivity described by means of the Drude model, ε is the dielectric constant, (IB) is the interband effect, , ε_{Au} is the relative permittivity of gold, ε_{α} is the permittivity of the metals, ω is the Frequency, ω_D is the plasma frequency; $\Delta\varepsilon$ is the weighting factor, and Ω_L and Γ_L respectively, Stand for the oscillator strength and the spectral width of the Lorentz oscillators.

Table 1. Drude-valued Lorentz parameters.

Symbol	ε_∞	$\omega_D/2\pi$	$\gamma_D/2\pi$	$\Omega_L/2\,\pi$	$\Gamma_L/2\,\pi$	$\Delta\varepsilon$	Φ
Unit		(THz)					
Meaning		the plasma frequency	the damping frequency	oscillator strength	The spectral width	The permittivity at high frequency	
Drude-Lorentz	5.9673	2113.6	15.92	650.07	104.86	1.09	14.521

3. Endlessly Single Photonic Crystal Fiber (ESM-PCF)

The PCF indicates slight loss during the largest wavelength series (200 nm to above 2000 nm) while holding a near continuous mode field diameter. This kind is consistent with wholly famous fiber instruments and contains a typical 125 µm outside diameter. A SEM image of PCF is shown in Figure 1.

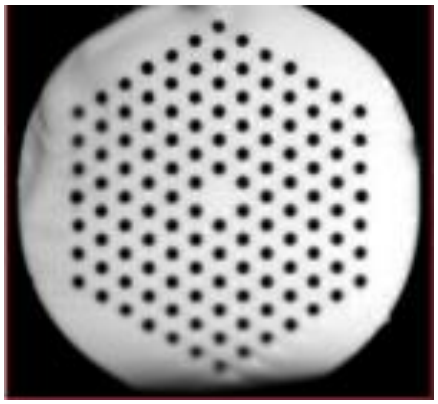

Fig.1: SEM image OF PCF.

4. Structural Technique and Analysis

NKT Inc.'s PCFs typically have an ESM fiber with an external diameter of 125µm. Figure 2 displays an illustration of the suggested sensor, produced by utilizing the COMSOL MULTPHYSICS software. Water is displaced into the air hole (d1). A plasmonic material like gold with a thickness of 50nm covers the air hole (d1). A Perfectly Matched Layer as an edge form has been utilized to absorb the scattering lights to the fiber surface; PML is a circular cover with a thickness of 12µm in the suggested design. Convergence tests also were concluded, and improved with mesh size and the PML thickness for additional precise effects.

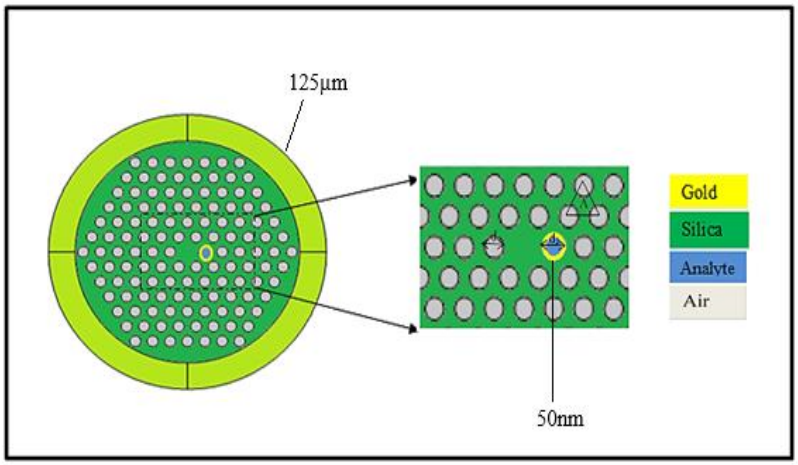

Fig. 2: 2D Cross-sectional observation of the suggested sensor.

5. Results and Discussion

For a specific wavelength, at a given temperature resonance is produced during the phase corresponding to core guiding mode and the Surface Plasmon Polariton mode. Figure (3) shows the electrical-filed distribution for (a) core-guided mode phase-matching condition and (b) SPP mode (y-polarized), respectively, at n_a =1.3266 and t_{Au} =50nm. In addition, Fig (4) illustrates the dispersion relation for y-polarizations around the resonant wavelength among the fundamental core mode and the second SPP mod. The confinement loss of the propagation mode is likewise displayed by this form (red line). There is a significant loss peak at the λ_{res} of 740 nm, where the 2ndSPP mode cross and essential mode were shown by the core. Consequently, the SPP mode obtains the most energy from the fundamental core mode.

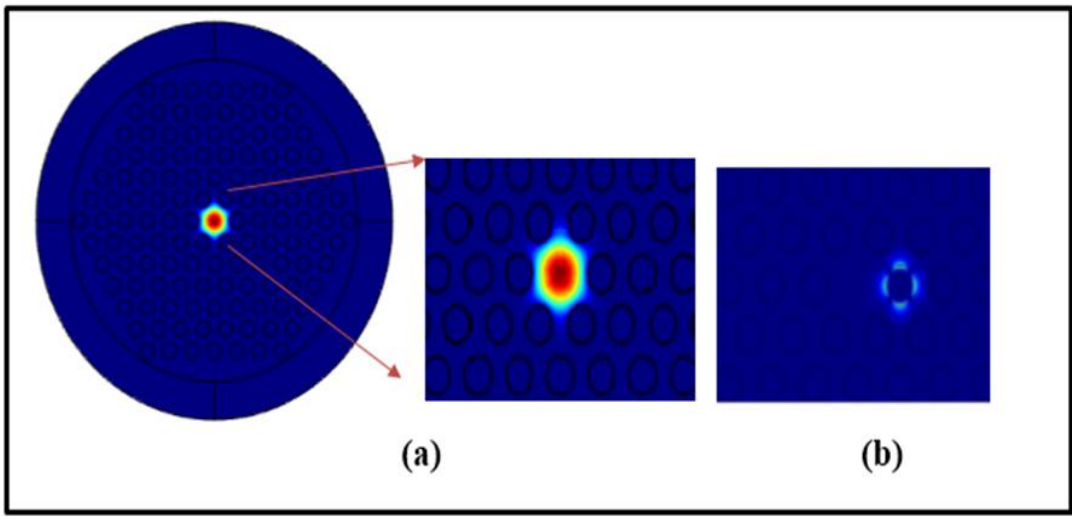

Fig. 3: Electric field distribution at the (a) core-guided mode phase-matching condition, and (b) SPP mode (y-polarized), respectively, at n_a=1.3266 and t_{Au}=50nm.

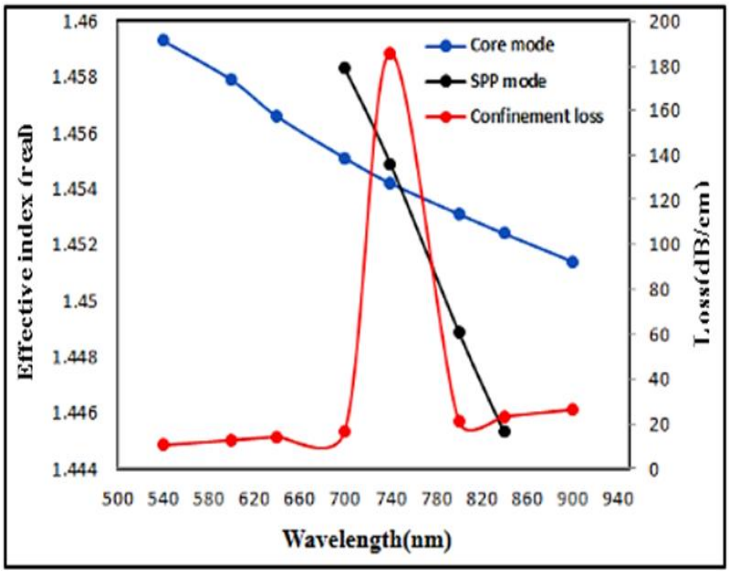

Fig. 4: Dispersion relation of the core-guided mode (blue), SPP mode (black), and loss spectrum (red) at na =1.3266 and t_{Au}=50nm.

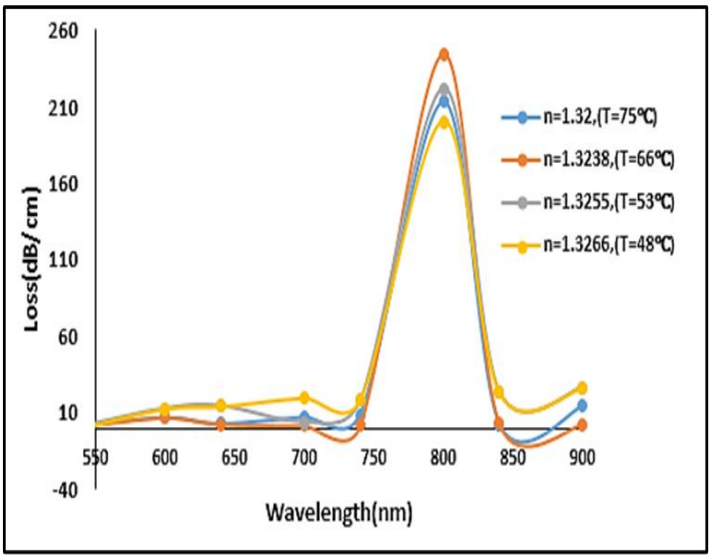

Fig. 5: The confinement loss spectrum of the suggested PCF SPR sensor difference with rise water RI from 1.32 to 1.3266 when temperature ranges from 48 °C to 75 °C.

The Refractive Index (RI) of water at different temperatures can be calculated by [32]:

$$n=n_o+ dn/dT \quad (T-T_o) \qquad (3)$$

Where n_o is the RI of the water at room temperature T_o and (dn/dT) is the thermo-optic coefficient, (dn/dT) of water is (−1.12 * 10^ (-4)/◦C) and (T) is the temperature increasing with water boiling [33]. We provide loss spectra for the core modes throughout the λspectrum of (540–900 nm) for the various RI of the water in order to investigate the RI sensitivity of the sensor. When the temperature rises from 48 °C to 75 °C, as displayed in Figure 5 the peak loss reduces unhurriedly. This is due to a poorer coupling efficiency caused by a larger variance between the Plasmon mode and core guided and a decreased n_{eff} of the Plasmon mode that varies the phase corresponding point.

As shown in Figure 5, the RI of water will reduce as temperature rises. To study the effect of varying refractive indices on the investigated sensor performance, the air hole on the right side of the photonic crystal fiber core was infiltrated with water. The refractive indices (na) of water vary from 1.32 to 1.3266 at a temperature field from 75 °C to 48 °C, Figure (5) shows confinement loss for the water refractive index extending from 1.32 to 1.3266. It was noted that the confinement loss was increased significantly with refractive index and this was because of the decrease in the refractive index difference between the core guided mode and SPP mode. Both wavelength methods amplitude interrogation can be utilized to measure the proposed sensor's implementation. Eq. 4 utilized to calculate the wavelength sensitivity [3]:

$$S_W(\lambda) = \frac{\Delta\lambda_{peak}}{\Delta n_a} \quad (4)$$

Δn_a and $\Delta\lambda_{peak}$ specify the variation in the analyte refractive index and the resonant peaks, correspondingly. Analytes with a refractive index of 1.32, 1.3238, and 1.3255 would be detected by the suggested sensor, and the wavelength sensitivity of an average of 526.3 nm/RIU, 1176.4 nm/RIU and 1818 nm/RIU can be achieved according to Eq. 4. The resolution of the sensor, which determines how well it detects even minute variations in the water RI, is another important consideration. Sensor resolution was determined using Eq. 5 [3]:

$$R = \frac{\Delta na \times \Delta\lambda min}{\Delta\lambda peak}\ [RIU] \quad (5)$$

Where $\Delta\lambda_{peak}$ is the greatest resonant wavelength peak shift, Δn_a is the difference in the refractive index of water, and $\Delta\lambda$min is the lower spectral resolution.2.75*10^(-5) RIU was the maximum resolution, assuming Δna = 0.0011, $\Delta\lambda$min = 0.1, and $\Delta\lambda$peak = 4 nm.

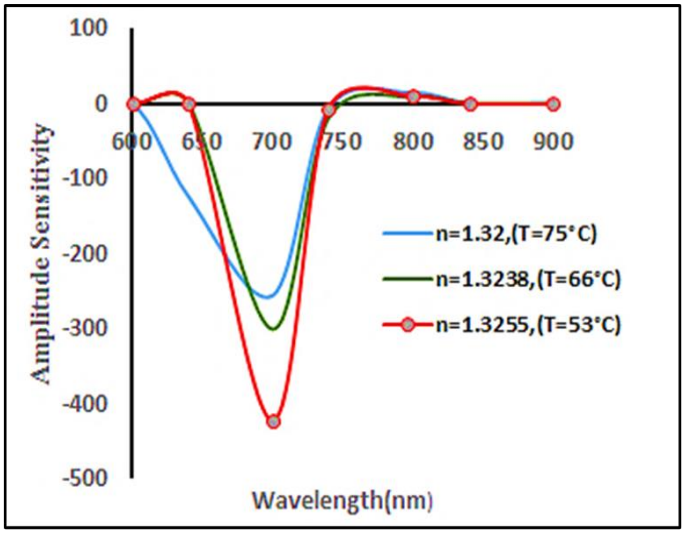

Fig. 6: Amplitude sensitivity relative to wavelength when RI increases from 1.33 to 1.3266.

To get the sensor's amplitude sensitivity, utilize Eq(6) [3]:

$$S_A(\lambda) = -\frac{1}{\alpha(\lambda,n_a)}\frac{\partial\alpha(\lambda,n_a)}{\partial n_a}[RIU^{-1}] \quad (6)$$

The analyte's confinement loss at a given refractive index (RI) is represented by α (λ,na), whereas the difference in confinement loss between two refractive indices is shown by ∂α (λ,na). The amplitude sensitivity of various refractive indices is shown in Figure 6. The greatest amplitude sensitivity for analytes 1.32 to 1.3238, 1.3238 to 1.3255, and 1.3255 to 1.3266 is 255.656RIU^ (-1), 300.12RIU^ (-1) and 422.154 RIU^ (-1) correspondingly.

6. Conclusion

PCF was utilized to present a temperature sensor based on the SPR technique. The PCF core exhibited a notable Y-polarization direction confinement loss after a gold-coated circular air hole on the right side was filled with an analyte (water sample). When the peak of the transmission loss spectrum or the resonant wavelength λres coincides with the SPR sensor's resonant wavelength, the filled analyte may be detected. FEM was employed to examine the basic mode sensor settings. In the sensing range of 1.32 to 1.3266, the maximum resolution of 2.75*10^ (-5) RIU and the amplitude sensitivity of 422.154 RIU^ (-1) were obtained. Due to its great sensitivity, the sensor is useful for biological and chemical sensing applications in the environment, such as detecting heavy metals in water. This sensor measures and detects a number of physical parameters, including chemical composition, strain, temperature, and pressure.

References

[1]E. Khatar and S. S. Bassam, "Surface Plasmon Plastic Optical Fiber Resonance with Multi-Layer as Chemical Sensor", Iraqi J. Phys. 19, 51.(2021)
[2] F. F Abbas, and S. S. Ahmed, "Photonic crystal fiber pollution sensor based on surface plasmon resonance", Iraqi Journal of Science, 658-667.(2023)
[3]G. M.Jassam, and S.S. Ahmed, "D-shaped photonic crystal fiber toxic metal ions (arsenic) sensor based on surface plasmon resonance", Iraqi Journal of Physics, 21(2), 91-98.(2023)
[4] G. M.Jassam and S. S. Ahmed, "Estimating concentration of toxic ions Arsenic in water by using Photonic Crystal Fiber based on Surface Plasmon Resonance (SPR)". Baghdad Science.(2023).
[5] F. F. Abbas and S. S. Ahmed, "Photonic crystal fiber pollution sensor based on the surface plasmon resonance technology", Baghdad Science Journal, 20(2), 0452-0452.(2023)
[6] M. J.Abd Alkareem, and S. S. Ahmed, "Surface Plasmon Resonance (SPR)-Based Multimode Optical Fiber Sensors for Electrical Transformer Oil Aging Detection", Iraqi Journal of Physics, 21(4), 84-91.(2023)
[7]H.Yang ,M. Liu,Y.Chen, L.Guo, G.Xiao, H.Liu, and L.Yuan,"Highly sensitive graphene-Au coated plasmon resonance PCF sensor", Sensors. 21(3), 818.(2021)
[8] P.Singal, and M. Kiroriwal ,"Performance Analysis of Gold-Coated Plasmonic Photonic Crystal Fiber Biosensor", In 2021 International Conference on Circuits, Controls and Communications (CCUBE) (pp. 1-4). IEEE(2021)
[9]M. J.Abd-ALhussain, B. G. Rasheed, and M. A. Fakhri,"Solid-core photonic crystal fiber-based nanolayer glucose sensor",Journal of Optics, 1-13.(2023)
[10] G. M. Jassam, S.S Ahmed, "Acetic acid concentration estimation using plastic optical fiber sensor-based surface plasmon resonance", Iraqi J. Phys. 17, 11.(2019)
[11]L.Liu, S.Deng, J.Zheng, L.Yuan, H.Deng and C. Teng, "An enhanced plastic optical fiber-based surface plasmon resonance sensor with a double-sided polished structure Sensors", 21, 1516.(2021)
[12]C.Odacı, and U.Aydemir, "The surface plasmon resonance-based fiber optic sensors: A theoretical comparative study with 2D TMDC materials",Results in Optics, 3, 100063.(2021)
[13]M.F.Sultan, A.A. Al-Zuky, and S.A.Kadhim, "Surface plasmon resonance based fiber optic sensor: theoretical simulation and experimental realization" ,Al-Nahrain J. Sci. 21, 65.(2018)
[14]G.Opoku, I.Danlard, A.Dede, and E. K.Akowuah, "Design and numerical analysis of a circular SPR based PCF biosensor for aqueous environments", Results in Optics, 12, 100432.(2023)
[15]C.Liu, J.Wang, F.Wang, W.Su, L.Yang, J.Lv, and P. K. Chu, "Surface plasmon resonance (SPR) infrared sensor based on D-shape photonic crystal fibers with ITO coatings" ,Optics Communications, 464, 125496(2020)
[16] X.Yan, Y.Wang, T.Cheng, and S.Li, "Photonic crystal fiber SPR liquid sensor based on elliptical detective channel".Micromachines. 12, 408.(2021)
[17]M. A.Mollah, S. R.Islam, M.Yousufali, L. F.Abdulrazak, , M. B.Hossain, and I. S.Amiri, "Numerical study of circularly slotted highly sensitive plasmonic biosensor: a novel approach",Results in Physics, 16, 102966.(2020)
[18]H. P.Li,J. Ruan, X. Li, G. Y.Wei, and T.He, "High-sensitivity temperature sensor based on surface plasmon resonance photonic crystal fiber" ,Progress In Electromagnetics Research . 116, 11.(2023)
[19] A. K.Paul, M. A.Mollah, M. Z.Hassan, N.Gomez-Cardona, and E.Reyes-Vera, "Graphene-coated highly sensitive photonic crystal fiber surface plasmon resonance sensor for aqueous solution: Design and numerical analysis",In Photonics. 8, 155 MDPI.(2021)

[20] N. S. Rahim, S. S. Bassam, "Estimating sugar concentration in human blood serum using Surface Plasmon Resonance (SPR) –based optical fiber sensor", Iraqi J. Phys. 17, 41.(2019)
[21] M. H.Salman, H. K.Muhammad and H. A.Yasser, "Effects of holes radius on plasmonic photonic crystal fiber sensor with internal gold layer",Periodicals of Engineering and Natural Sciences, 8, 1288 .(2020)
[22] N.Sakib, W.Hassan, Q. M.Kamrunnahar,M. Momtaj, and T.Rahman, "Dual core four open channel circularly slotted gold coated plasmonic biosensor" ,Optical Materials Express, 11, 273 .(2021)
[23] M.lA Mahfuz, M. A.Hossain, E.Haque, N. H.Hai, Y.Namihira, and F.Ahmed, "Dual-core photonic crystal fiber-based plasmonic RI sensor in the visible to near-IR operating band", IEEE Sensors Journal, 20, 7692.(2020)
[24] N. S. Rahim, S. S. Ahmed, and M. F. Sultan, "Optical fiber biomedical sensor based on surface plasmon resonance", Iraqi J. Sci. 61, 1650-1656.(2020)
[25] G. M. Jassam, S. S. Alâ, and M. F. Sultan, "Fabrication of a chemical sensor based on surface plasmon resonance via plastic optical fiber", Iraqi J. Sci. 61, 765.(2020)
[26] W.Yong, S.Yudong, L.Chunlan, L.Lu, Z. Zongda and Z. Yonghui, "Micro-displacement optical fiber sensor based on surface plasmon resonance", Laser Optoelectron. Prog. 55, 040606.(2018)
[27] Y.Yang, Y.Qin, X. Lu, and Y.Zeng, "High-sensitivity three-core photonic crystal fiber sensor based on surface plasmon resonance with gold film coatings",Japanese Journal of Applied Physics, 60, 122002.(2021)
[28]A.S.H.Rabee, M.F.O.Hameed, A.M.Heikal and S.Obayya, "Highly sensitive photonic crystal fiber gas sensor" ,Optik, 188, 78.(2019)
[29] Q.H.Chen, , J.H.Liu, H.F.Luo, Y.X.He, J.Luo and F.Wang, "A liquid refractive index measurement system based on surface plasma resonance" ,Acta Opt. Sin. 35, 166.(2015)
[30] K.M.McPeak, S. V.Jayanti, S. J.Kress, S.Meyer, S.Iotti, A.Rossinelli, and D. J. Norris, ACS photonics, 2, 326.(2015)
[31] R. Otupiri, E. K. Akowuah, S. Haxha, H. Ademgil, F. AbdelMalek, and A. Aggoun, "A novel birefrigent photonic crystal fiber surface plasmon resonance biosensor",IEEE Photon. J., 6, 6801711 (2014)
[32] X. C. Yang, Y.Lu, B. L.Liu and J. Q.Yao, "Temperature sensor based on photonic crystal fiber filled with liquid and silver nanowires", IEEE Photonics Journal, 8, 1.(2016)
[33] P. R. Prasad, S. K.Selvaraja and M.Varma, "Thermo-optic coefficient measurement of liquids using silicon photonic microring resonators" ,arXiv preprint arXiv,1710.03605 .(2017)

مستشعر درجة حرارة بالألياف البلورية الضوئية استنادًا إلى رنين البلازمون السطحي (SPR)

نماء سالم رحيم * ، سؤدد سلمان احمد

قسم الفيزياء، كلية العلوم، جامعة بغداد، العراق، بغداد

*البريد الالكتروني للباحث: : namaasalem652@gmail.com

الخلاصة:تم تحضير ودراسة مستشعرات الألياف البلورية الضوئية (PCF) المستنده على رنين البلازمون السطحي مع طبقة من الذهب في هذا البحث للكشف عن درجة حرارة البيئية. يتم استخدام طريقة العناصر المحدودة لزيادة معلمة الهندسة الحرجة.ثقب الهواء الموجود على الجانب الأيمن من قلب الPCF مغطاة بمادة ذهبية بلازمونية مستقرة كيميائيًا يبلغ سمكها 50 نانومتر. كان للالياف البلورية الضوئية ذات الفتحات الهواء الدائرية المطلية بالذهب والمملوءة بعينات الماء خسائر كبيرة في الحصرفي اتجاه الاستقطاب y. عندما ترتفع درجة الحرارة من 48 درجة مئوية إلى 75 درجة مئوية فإن معامل الانكسارللماء سوف تنخفض.تم إجراء التحليل العددي للمتحسس المقترح باستخدام طريقة العناصر المحدودة.تم استخدام المحاكاة باستخدام برنامج COMSOL لحساب معلمات الأداء مثل حساسية السعة وحساسية الطول الموجي والدقة. تشير النتائج إلى أن فتحة الهواء المغطاة بـ (الذهب) تعمل بمثابة تغذية استشعار (SPR) لاستشعار معامل انكسار الماء.في مدى استشعار (1.32-1.3266), كانت حساسية السعة 422.154(-1) والدقة⟦ 10*6⟧^(-6) RIU.